

Towards Trustworthy Healthcare AI: Attention-Based Feature Learning for COVID-19 Screening With Chest Radiography

Kai Ma^{*1} Pengcheng Xi^{*1,2} Karim Habashy^{1,2} Ashkan Ebadi^{1,2} Stéphane Tremblay² Alexander Wong¹

Abstract

Building AI models with trustworthiness is important especially in regulated areas such as healthcare. In tackling COVID-19, previous work uses convolutional neural networks as the backbone architecture, which has shown to be prone to overcaution and overconfidence in making decisions, rendering them less trustworthy — a crucial flaw in the context of medical imaging. In this study, we propose a feature learning approach using Vision Transformers, which use an attention-based mechanism, and examine the representation learning capability of Transformers as a new backbone architecture for medical imaging. Through the task of classifying COVID-19 chest radiographs, we investigate into whether generalization capabilities benefit solely from Vision Transformers’ architectural advances. Quantitative and qualitative evaluations are conducted on the trustworthiness of the models, through the use of “trust score” computation and a visual explainability technique. We conclude that the attention-based feature learning approach is promising in building trustworthy deep learning models for healthcare.

1. Introduction

COVID-19 has affected lives around the world and continues with Omicron XE variant and possible future mutants, variants or recombinants. Screening and monitoring of patients regarding the virus have never been more important. In dealing with the pandemic, building AI models with trust is an important topic for researchers, clinicians, and patients.

The medical image analysis field has been dominated by

^{*}Equal contribution ¹Faculty of Engineering, University of Waterloo, Waterloo, Ontario, Canada ²Digital Technologies Research Centre, National Research Council Canada, Ottawa, Ontario, Canada. Correspondence to: Kai Ma <k78ma@uwaterloo.ca>, Pengcheng Xi <pengcheng.xi@nrc-cnrc.gc.ca>.

deep Convolutional Neural Networks (CNN). A drawback of deep CNNs is that they are often overly cautious for correct predictions of the minority class, while exhibiting overconfidence for incorrect predictions of the majority class (Esposito et al., 2021). This problem is significant in medical image analysis, considering that results with low trust may lead to serious medical consequences.

Recent innovations in computer vision (CV) have shown that Vision Transformer models can outperform CNNs. The models are based on an attention mechanism, first introduced for natural language processing (NLP) (Vaswani et al., 2017). In (Dosovitskiy et al., 2020), the authors introduced the original Vision Transformer named ViT, which yielded modest performance when trained on ImageNet (Deng et al., 2009), with limited generalization capabilities (Touvron et al., 2020). Based on this architecture, a hierarchical variant named Swin Transformer (Liu et al., 2021b) was proposed to compute representations with shifted windows. The hierarchical architecture allows flexibility to model at various scales besides computational efficiency. The Swin Transformer has achieved state-of-the-art (SOTA) performance on tasks including image classification, object detection, and semantic segmentation. It can therefore serve as a general-purpose backbone for computer vision.

There is potential for applying Transformers to medical image analysis. CNNs have inductive biases, such as locality and translational equivariance, baked into their architectures; however, Transformers use self-attention to establish relationships between long-range elements and can attend over different regions of an image, leading to the integration of information across the entire image. When radiologists or doctors read chest X-rays, they tend to read different parts of the images and combine features for reporting and diagnosis (Cleverley et al., 2020), which is analogous to a Transformer’s self-attention. Furthermore, the attention mechanism used in Transformers has an improved ability to preserve spatial information, which can lead to improved performance and trust in models (Raghu et al., 2021).

In this study, we propose an attention-based model architecture to improve model trustworthiness, through leveraging the unique strength of Vision Transformers. For validations, we choose ResNet-50 (He et al., 2015) and DenseNet-121

(Huang et al., 2016) for comparison as they are commonly used as baselines and have also demonstrated good performance on similar tasks (Farooq & Hafeez, 2020; Ayyar et al., 2021). The vanilla Swin Transformer is chosen as a representative Vision Transformer model, as it represents a step up from the modest original ViT but is also not so architecturally advanced as to lead to an unfair comparison.

We study model trustworthiness with quantitative measures and qualitative evaluations. Using CNNs or Transformers as backbones, the models are pre-trained on ImageNet-1K and fine-tuned on COVIDx (Wang et al., 2020), a chest X-ray dataset which combines several well-known public data repositories such as RSNA (Chowdhury et al., 2020; Rahman et al., 2021) and ActualMed (Chung, 2020). We adopt a novel trust score introduced in (Wong et al., 2020) and an explainability technique named Ablation-CAM (Desai & Ramaswamy, 2020). Experimental results indicate that attention-based models are consistently more trustworthy than CNN counterparts with similar performance. To our best knowledge, this is the first evaluation of Vision Transformers using the quantitative trust scores, indicating a feasibility of building trustworthy AI models for healthcare.

2. Literature Review

Vision Transformers (ViT) were first introduced in (Dosovitskiy et al., 2020), using image patches with positional embeddings. The key mechanism behind the architecture is known as “attention”, which aims to emphasize important parts of input data while diminishing others for the purpose of imitating human cognitive attention. With the inaugural success of the ViT models, several variations have followed. A notable development is the Swin Transformer (Liu et al., 2021b), which uses a shifted windowing scheme: by attention to local windows, it allows for cross-window connections and implements a merging layer to combine image patches. It has therefore achieved high efficiency and exceptional performance, surpassing SOTA CNNs.

Other developments, including CoAtNet (Dai et al., 2021), MaxViT (Tu et al., 2022), and SwinV2 (Liu et al., 2021a), have consistently shown high performance on ImageNet benchmarks, beating previous approaches. These models are available in different versions, while pre-trained on different datasets. For example, the Swin Transformer has variants pre-trained on either ImageNet-1K or ImageNet-22K (Deng et al., 2009), base version Swin-B, small versions Swin-T and Swin-S, and large version Swin-L (Liu et al., 2021b)), as well as using different image sizes.

COVID-19 causes the density of the lungs to increase, often presenting as whiteness in the lungs when seen in chest radiographs. This may obscure normal lung markings, resulting in a “ground glass” pattern (Cleverley et al., 2020).

In severe cases, lung markings can be completely lost due to whiteness, which is called “consolidation”. Furthermore, coarse, horizontal white lines can appear, which are termed “peripheral linear opacities”. When examining chest radiographs for COVID-19, radiologists review images systematically, including examining the heart, lungs, ribs, diaphragm, and mediastinum for evidence of ground glass opacity, peripheral linear opacities, or consolidation. While these are commonly used as evidence for diagnosis, changes due to COVID-19 can be subtle or even absent.

Deep learning metrics are well-documented for evaluating performance, efficiency, and explainability (Lin et al., 2019; Canziani et al., 2016; Wong, 2018). In contrast, model trustworthiness is a relatively new area of interest. Most approaches focus on quantifying trust for a prediction made on a single data sample, using uncertainty estimations (Titeny et al., 2018; Geifman et al., 2018) or agreement with a modified nearest-neighbour classifier (Jiang et al., 2018). However, these methods are often difficult to interpret and have high complexity (Kendall & Gal, 2017).

To address the above issue, authors in (Wong et al., 2020) introduced the concept of “question-answer trust”, where the trustworthiness of a deep neural network is determined by its behaviour under correct and incorrect answer scenarios. To that end, the question-answer trust fundamentally penalizes undeserved confidence while rewarding well-placed confidence. A simple scalar “trust score” metric is introduced to put question-answer trust to practice — a higher trust score indicates a more trustworthy model. This trust score method was tested experimentally with ImageNet, achieving insightful results; furthermore, it has been adopted for medical applications (Meng et al., 2022; Parra et al., 2021), showing its validity and applicability to the task at hand.

For model explainability, a common approach is to locate regions in a given input image that are used by the model for classifications. There is existing literature on this topic for Transformers in the context of medical imaging (Chetoui & Akhloufi, 2022); however, the authors use attention maps based on self-attention score, which is specific to Transformers and does not apply to CNNs, and no comparison is done between the two.

We aim to use an approach that is applicable to both CNNs and Transformers. One example approach for producing localization maps is Grad-CAM (Selvaraju et al., 2016), which uses gradients flowing into the final layer. Due to this focus on the final layer, Grad-CAM can be ineffective for Transformer architectures, which have relatively uniform representations across all layers (Raghu et al., 2021). Furthermore, Grad-CAM can be prone to low-quality visualizations as a result of gradient saturation (Desai & Ramaswamy, 2020). Instead, another approach named Ablation-CAM (Desai & Ramaswamy, 2020) solves these problems by us-

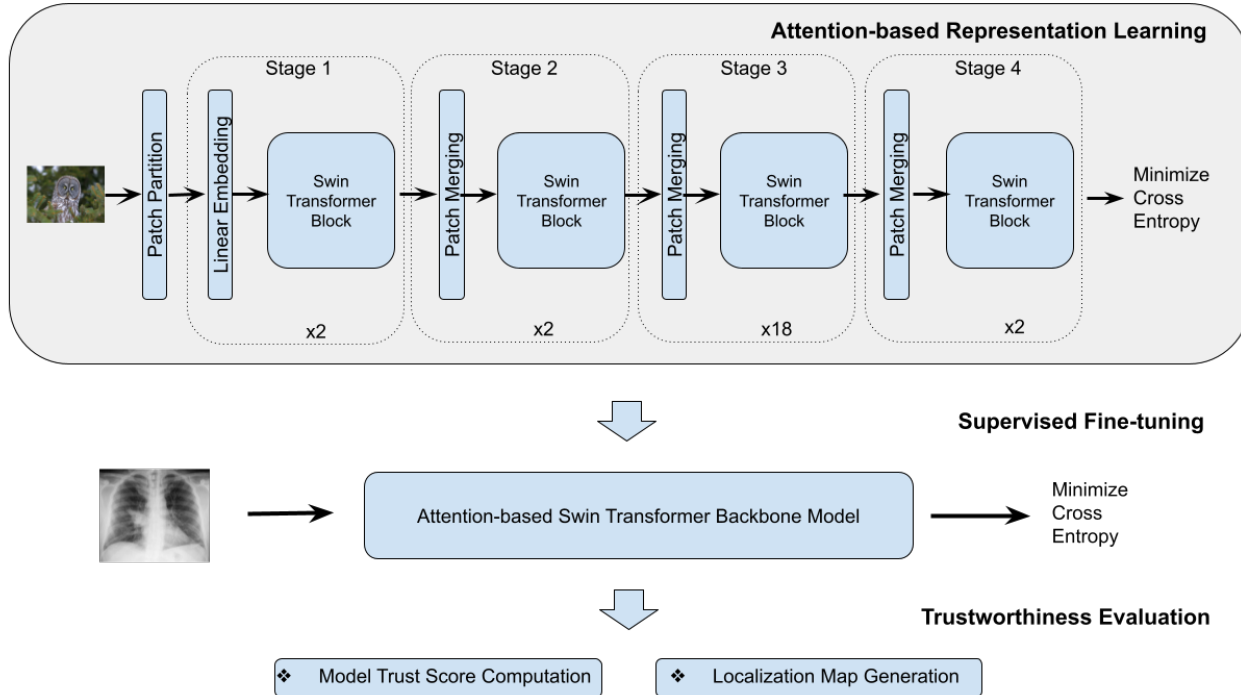


Figure 1. Model architecture and fine-tuning pipeline.

ing ablation analysis instead of gradients, resulting in immunity to saturation. As such, Ablation-CAM is able to provide visualizations that are more complete and trustworthy, and suitable for both Transformers and CNNs, demonstrating better performance than Grad-CAM for our purposes.

3. Methodology

Our methodology is motivated by the unique architecture of Vision Transformers and their capability of creating models with improved trustworthiness. In particular, Swin Transformer (Liu et al., 2021b) was introduced to prove its capability of serving as a general-purpose backbone for computer vision. It is a hierarchical transformer which computes representations with shifted windows, bringing efficiency by limiting self-attention computation to non-overlapping local windows. Its key design element lies in the shift of the window partitions between consecutive self-attention layers.

3.1. Model Architecture

We propose the model architecture in Fig. 1, where we follow a transfer learning approach (Kolesnikov et al., 2019). We first conduct attention-based representation learning to build the backbone transformer model. We then freeze the encoder part and only fine-tune the classifier parts of the Swin Transformer models using the COVIDx data set. We specifically use the Swin-Base Transformer model, hence-

forth referred to as “Swin-B”. Models are created using TorchVision (Paszke et al., 2019), then modified such that the final fully connected layer is replaced with a single output neuron for binary classification. To produce probability distributions, a sigmoid layer is applied over the raw logits.

Validation is conducted after each training epoch and a classification threshold is calculated by maximizing validation F1-score. The model achieving the best validation accuracy is saved and then evaluated on the unseen test split. Finally, trustworthiness of the saved model is evaluated by calculating a “trust score” for the positive class according to the method described in (Wong et al., 2020). This metric expresses model trustworthiness by rewarding well-placed confidence and penalizing undeserved overconfidence. A higher trust score indicates that a model is more trustworthy.

3.2. Trust Score Computation

Trust scores are computed using the method introduced in (Wong et al., 2020). Given a question x , an answer y given by a model M , such that $y = M(x)$, and z representing the correct answer to x , we use $R_{y=z|M}$ to denote the space of all questions where the answer y given by model M matches the correct answer z . Similarly, $R_{y \neq z|M}$ is used to denote the space of all questions where y does not match the correct answer. The confidence of M in an answer y to question x is denoted as $C(y | x)$. Thus, the *question-answer trust* of an answer y given by model M for a question x , with

knowledge of the correct answer z , is defined as

$$Q_z(x, y) = \begin{cases} C(y | x)^\alpha, & \text{if } x \in R_{y=z|M} \\ (1 - C(y | x))^\beta, & \text{if } x \in R_{y \neq z|M}, \end{cases}$$

with α and β denoting reward and penalty coefficients.

In practical usage with our models, we first calculate an optimal threshold value by maximizing F1-score on the validation split. Samples are individually passed through the model; outputs below the threshold are predicted to be negative, while outputs above the threshold are predicted to be positive. We then normalize outputs, such that negative predictions are scaled between 0 and 0.5 and positive predictions are scaled between 0.5 and 1. This allows us to represent model confidence, which is then used to compute a *trust score* according to the method introduced above. To equally reward well-placed confidence and undeserved overconfidence, we use $\alpha = \beta = 1$. Finally, an overall positive class trust score for the model is determined by calculating the mean of all individual scores for all of the positive samples in the unseen test split.

4. Experimental Results

4.1. Dataset

For a fair comparison, all the models are pre-trained on the same dataset ImageNet-1K (Deng et al., 2009). We fine-tune the models on COVIDx (Version 9B) (Wang et al., 2020), which consists of 30,482 chest radiographs with annotations on having COVID-19 or not (Table 1). The dataset has a defined testing subset of 400 images, which is used for evaluating the fine-tuned models. Within the training split, 10% of the images are sampled for validations.

Table 1. Data split for COVIDx V9B

SPLIT	NEGATIVE	POSITIVE	TOTAL
TRAIN	13,992	15,950	30,482
TEST	200	200	400

4.2. Experiment Setups

Input images are resized and center cropped to 224×224 and normalized, with random horizontal flipping as the only data augmentation being implemented. More data augmentations, while being effective for improving model performance (Touvron et al., 2020), will complicate the strict architecture-based comparison we are conducting.

Cross-entropy loss with SGD optimizer is used with a weight decay of $1e - 4$ and momentum of 0.9. Initial learning rates are set for the different number of training epochs (Table 2). Cosine annealing learning rate decay is used.

Table 2. Initial learning rates by number of training epochs

EPOCHS	30	50	100	200
INITIAL LR	$5e-4$	$5e-4$	$3e-4$	$1e-4$

4.3. Model Performance and Trust

To establish a baseline result for the dataset, we fine-tune ResNet-50 and DenseNet-121 for 200 epochs and compute trust scores. Our best model fine-tuned on the Swin Transformer backbone is trained with 200 epochs. In Tables 3, 4, and 5, we also include the precision, sensitivity, and trust scores of models trained with less epochs.

Table 3. Precision scores on the unseen COVIDx V9B test split. The best results in each class are bolded.

MODEL	NEGATIVE	POSITIVE
RESNET (200 EPOCHS)	0.952	1.000
DENSENET (200 EPOCHS)	0.948	0.995
SWIN-B (30 EPOCHS)	0.926	1.000
SWIN-B (50 EPOCHS)	0.935	1.000
SWIN-B (100 EPOCHS)	0.930	1.000
SWIN-B (200 EPOCHS)	0.952	1.000

Table 4. Sensitivity scores on the unseen COVIDx V9B test split. The best results in each class are bolded.

MODEL	NEGATIVE	POSITIVE
RESNET (200 EPOCHS)	1.000	0.950
DENSENET (200 EPOCHS)	0.995	0.945
SWIN-B (30 EPOCHS)	1.000	0.920
SWIN-B (50 EPOCHS)	1.000	0.930
SWIN-B (100 EPOCHS)	1.000	0.925
SWIN-B (200 EPOCHS)	1.000	0.950

From the results in Tables 3 and 4, we see that the Swin-B models are consistently matching ResNet-50 and surpassing DenseNet-121 for the precision metric of the positive class and the sensitivity metric of the negative class. These metrics are especially meaningful in the context of medical imaging: a higher sensitivity score in the negative class implies that there are less false-positives. Moreover, the Swin-B model (200-epoch) was able to match the baseline ResNet-50 model in both classes for precision and sensitivity. This highly successful fine-tuned Swin-B model will be made publicly available upon acceptance of this work.

While the ResNet-50 model outperforms some Swin-B models (trained for less than 200 epochs) in terms of precision

Table 5. Trust scores calculated from each experiment on the positive class. The best result is bolded.

MODEL	TRUST SCORE
RESNET (200 EPOCHS)	0.923
DENSENET (200 EPOCHS)	0.922
SWIN-B (30 EPOCHS)	0.943
SWIN-B (50 EPOCHS)	0.959
SWIN-B (100 EPOCHS)	0.954
SWIN-B (200 EPOCHS)	0.963

and recall, the results presented in table 5 indicate that Swin-B models consistently achieve significantly higher trust scores than both ResNet-50 and DenseNet-121. The aforementioned Swin-B model (200-epoch) achieved the highest trust score out of all models. Thus, it is shown that Swin Transformers can achieve competitive performance to ResNet-50 and surpass DensNet-121 while being significantly more trustworthy.

We conducted additional experiments to study representation learning capabilities of vanilla Swin Transformers. Specifically, fine-tuning was performed on a smaller variant of the Swin Transformer, the Swin-Tiny (Swin-T), and it is compared with the Swin-B model when both are fine-tuned for 50 epochs. Results are listed in Tables 6, 7, and 8. Although the Swin-T model is lackluster in terms of model performance, it achieved a trust score similar to Swin-B model, which is much higher than the ResNet-50 and DenseNet-121 baselines. This strengthens our conclusion that the Transformer architecture itself can contribute to model trustworthiness.

Table 6. Precision scores on the unseen COVIDx V9B test split.

MODEL	NEGATIVE	POSITIVE
SWIN-T	0.913	1.000
SWIN-B	0.935	1.000

Table 7. Sensitivity scores on the unseen COVIDx V9B test split.

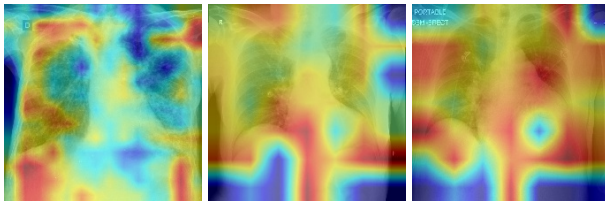
MODEL	NEGATIVE	POSITIVE
SWIN-T	1.000	0.905
SWIN-B	1.000	0.930

4.4. Localization Map Analysis

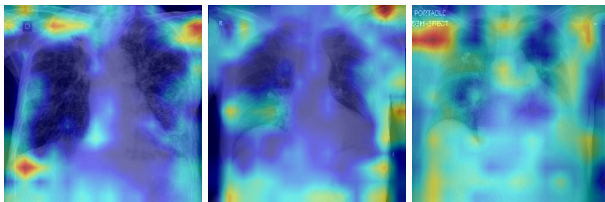
We produce localization maps by computing Ablation-CAMs for our models, applied to over 100 images from



(a) Original chest radiographs for positive COVID-19 samples



(b) Swin-B 200-epoch Ablation-CAM



(c) ResNet-50 200-epoch Ablation-CAM

Figure 2. Swin-B and ResNet-50 Ablation-CAMs for 3 selected COVID-positive chest X-rays. ResNet-50 is chosen as a representative because it produced better results and localization maps than Densenet-121. Warm colors (red, orange) indicate high importance, cold colors (blue, green) indicate lower importance.

the COVIDx test split. These maps highlight image regions deemed important by the model for classifications. Figures 2a and 2b show three example COVID-positive images and localization maps computed on the Swin-B model (200-epoch). Figure 2c shows corresponding maps produced by the ResNet-50 baseline model on the same images.

The localization maps produced by Swin Transformers highlight the lung area, successfully focusing on the ground glass pattern, consolidation and peripheral linear opacities used by human doctors for diagnosis (Cleverley et al., 2020). In contrast, maps produced by the ResNet-50 are less successful, highlighting irrelevant areas such as shoulders and arms, sometimes missing the lungs entirely.

5. Conclusion

In the context of building healthcare AI models, we propose an attention-based model architecture to improve model trustworthiness, an important topic for researchers, clinicians, and patients. We have compared the effectiveness of Transformer and CNN models used as backbone architectures for screening COVID-19 patients using chest X-ray

Table 8. Trust scores calculated on the positive class.

MODEL	TRUST SCORE
SWIN-T	0.954
SWIN-B	0.959

images. Through quantitative and qualitative evaluations, we demonstrate that the attention-based models are capable of matching CNN models in performance, while achieving significantly higher trustworthiness. This advantage is further validated through localization maps, which highlight regions deemed important by the models. The Transformers are shown to be better at identifying medically relevant lung regions than CNNs. We conclude that the trustworthiness and performance obtained by the Transformers are due to their architecture improvements over the CNN counterparts; therefore, models built upon attention-based backbone architectures are promising for medical imaging tasks, including COVID-19 and other healthcare applications.

For further improvement, our future work includes fine-tuning with the larger “Swin-L” Transformer model. Moreover, experiments with different loss functions instead of standard cross-entropy loss, such as those designed for medical image analysis (Yuan et al., 2020), will be further studied to improve performance and trust. To test the generalization capability of the proposed approach, we plan to validate the pipeline on other datasets including SIIM-FISABIO-RSNA (Lakhani et al., 2021). Finally, while Transformer-based models are currently popular in the field of computer vision, innovations have not stopped for CNN models. We are interested in comparing Transformers to newer CNN models, such as ConvNeXt (Liu et al., 2022), which has achieved excellent results by incorporating Transformer-like characteristics into CNN architectures.

References

- Ayyar, M. P., Benois-Pineau, J., and Zemmari, A. A hierarchical classification system for the detection of covid-19 from chest x-ray images. In *2021 IEEE/CVF International Conference on Computer Vision Workshops (ICCVW)*, pp. 519–528, Los Alamitos, CA, USA, oct 2021. IEEE Computer Society. doi: 10.1109/ICCVW54120.2021.00064. URL <https://doi.ieeecomputersociety.org/10.1109/ICCVW54120.2021.00064>.
- Canziani, A., Paszke, A., and Culurciello, E. An analysis of deep neural network models for practical applications. *CoRR*, abs/1605.07678, 2016. URL <http://arxiv.org/abs/1605.07678>.
- Chetoui, M. and Akhloufi, M. A. Explainable vision transformers and radiomics for covid-19 detection in chest x-rays. *Journal of Clinical Medicine*, 11(11), 2022. ISSN 2077-0383. doi: 10.3390/jcm11113013. URL <https://www.mdpi.com/2077-0383/11/11/3013>.
- Chowdhury, M. E. H., Rahman, T., Khandakar, A., Mazhar, R., Kadir, M. A., Mahbub, Z. B., Islam, K. R., Khan, M. S., Iqbal, A., Al-Emadi, N., and Reaz, M. B. I. Can AI help in screening viral and COVID-19 pneumonia? *CoRR*, abs/2003.13145, 2020. URL <https://arxiv.org/abs/2003.13145>.
- Chung, A. Actualmed covid-19 chest x-ray data initiative, 2020. URL <https://github.com/agchung/Actualmed-COVID-chestxray-dataset>.
- Cleverley, J., Piper, J., and Jones, M. M. The role of chest radiography in confirming covid-19 pneumonia. *BMJ*, 370, 2020. doi: 10.1136/bmj.m2426. URL <https://www.bmj.com/content/370/bmj.m2426>.
- Dai, Z., Liu, H., Le, Q. V., and Tan, M. Coatnet: Marrying convolution and attention for all data sizes. *CoRR*, abs/2106.04803, 2021. URL <https://arxiv.org/abs/2106.04803>.
- Deng, J., Dong, W., Socher, R., Li, L.-J., Li, K., and Fei-Fei, L. ImageNet: A Large-Scale Hierarchical Image Database. In *CVPR09*, 2009.
- Desai, S. and Ramaswamy, H. G. Ablation-cam: Visual explanations for deep convolutional network via gradient-free localization. In *2020 IEEE Winter Conference on Applications of Computer Vision (WACV)*, pp. 972–980, 2020. doi: 10.1109/WACV45572.2020.9093360.
- Dosovitskiy, A., Beyer, L., Kolesnikov, A., Weissenborn, D., Zhai, X., Unterthiner, T., Dehghani, M., Minderer, M., Heigold, G., Gelly, S., Uszkoreit, J., and Houlsby, N. An image is worth 16x16 words: Transformers for image recognition at scale, 2020. URL <https://arxiv.org/abs/2010.11929>.
- Esposito, C., Landrum, G., Schneider, N., Stiefl, N., and Riniker, S. Ghost: Adjusting the decision threshold to handle imbalanced data in machine learning. *Journal of Chemical Information and Modeling*, vol. 61, no. 6, pp. 2623–2640:2623–2640, 2021. URL <https://doi.org/10.1021/acs.jcim.1c00160>.
- Farooq, M. and Hafeez, A. Covid-resnet: A deep learning framework for screening of covid19 from radiographs, 2020. URL <https://arxiv.org/abs/2003.14395>.

- Geifman, Y., Uziel, G., and El-Yaniv, R. Boosting uncertainty estimation for deep neural classifiers. *CoRR*, abs/1805.08206, 2018. URL <http://arxiv.org/abs/1805.08206>.
- He, K., Zhang, X., Ren, S., and Sun, J. Deep residual learning for image recognition, 2015. URL <https://arxiv.org/abs/1512.03385>.
- Huang, G., Liu, Z., and Weinberger, K. Q. Densely connected convolutional networks. *CoRR*, abs/1608.06993, 2016. URL <http://arxiv.org/abs/1608.06993>.
- Jiang, H., Kim, B., Guan, M. Y., and Gupta, M. To trust or not to trust a classifier, 2018. URL <https://arxiv.org/abs/1805.11783>.
- Kendall, A. and Gal, Y. What uncertainties do we need in bayesian deep learning for computer vision? *CoRR*, abs/1703.04977, 2017. URL <http://arxiv.org/abs/1703.04977>.
- Kolesnikov, A., Beyer, L., Zhai, X., Puigcerver, J., Yung, J., Gelly, S., and Houlsby, N. Big transfer (bit): General visual representation learning, 2019. URL <https://arxiv.org/abs/1912.11370>.
- Lakhani, P., Mongan, J., Singhal, C., Zhou, Q., Andriole, K. P., Auffermann, W. F., Prasanna, P., Pham, T., Peterson, M., Bergquist, P. J., and et al. The 2021 siim-fisabior-sna machine learning covid-19 challenge: Annotation and standard exam classification of covid-19 chest radiographs., Oct 2021. URL osf.io/532ek.
- Lin, Z.-Q., Shafiee, M. J., Bochkarev, S., Jules, M. S., Wang, X., and Wong, A. Do explanations reflect decisions? A machine-centric strategy to quantify the performance of explainability algorithms. *CoRR*, abs/1910.07387, 2019. URL <http://arxiv.org/abs/1910.07387>.
- Liu, Z., Hu, H., Lin, Y., Yao, Z., Xie, Z., Wei, Y., Ning, J., Cao, Y., Zhang, Z., Dong, L., Wei, F., and Guo, B. Swin transformer V2: scaling up capacity and resolution. *CoRR*, abs/2111.09883, 2021a. URL <https://arxiv.org/abs/2111.09883>.
- Liu, Z., Lin, Y., Cao, Y., Hu, H., Wei, Y., Zhang, Z., Lin, S., and Guo, B. Swin transformer: Hierarchical vision transformer using shifted windows. In *Proceedings of the IEEE/CVF International Conference on Computer Vision (ICCV)*, 2021b.
- Liu, Z., Mao, H., Wu, C., Feichtenhofer, C., Darrell, T., and Xie, S. A convnet for the 2020s. *CoRR*, abs/2201.03545, 2022. URL <https://arxiv.org/abs/2201.03545>.
- Meng, C., Trinh, L., Xu, N., Enouen, J., and Liu, Y. Interpretability and fairness evaluation of deep learning models on mimic-iv dataset. *Scientific Reports*, 12(1): 7166, May 2022. ISSN 2045-2322. doi: 10.1038/s41598-022-11012-2. URL <https://doi.org/10.1038/s41598-022-11012-2>.
- Parra, R., Ojeda, V., Vázquez Noguera, J. L., García-Torres, M., Mello-Román, J. C., Villalba, C., Facon, J., Divina, F., Cardozo, O., Castillo, V. E., and Matto, I. C. A trust-based methodology to evaluate deep learning models for automatic diagnosis of ocular toxoplasmosis from fundus images. *Diagnostics (Basel)*, 11(11):1951, October 2021.
- Paszke, A., Gross, S., Massa, F., Lerer, A., Bradbury, J., Chanan, G., Killeen, T., Lin, Z., Gimelshein, N., Antiga, L., Desmaison, A., Kopf, A., Yang, E., DeVito, Z., Raison, M., Tejani, A., Chilamkurthy, S., Steiner, B., Fang, L., Bai, J., and Chintala, S. Pytorch: An imperative style, high-performance deep learning library. In Wallach, H., Larochelle, H., Beygelzimer, A., d'Alché-Buc, F., Fox, E., and Garnett, R. (eds.), *Advances in Neural Information Processing Systems 32*, pp. 8024–8035. Curran Associates, Inc., 2019.
- Raghu, M., Unterthiner, T., Kornblith, S., Zhang, C., and Dosovitskiy, A. Do vision transformers see like convolutional neural networks? *CoRR*, abs/2108.08810, 2021. URL <https://arxiv.org/abs/2108.08810>.
- Rahman, T., Khandakar, A., Qiblawey, Y., Tahir, A., Kiranyaz, S., Abul Kashem, S. B., Islam, M. T., Al Maadeed, S., Zughaier, S. M., Khan, M. S., and Chowdhury, M. E. Exploring the effect of image enhancement techniques on covid-19 detection using chest x-ray images. *Computers in Biology and Medicine*, 132:104319, 2021. ISSN 0010-4825. doi: <https://doi.org/10.1016/j.compbio.2021.104319>. URL <https://www.sciencedirect.com/science/article/pii/S001048252100113X>.
- Selvaraju, R. R., Das, A., Vedantam, R., Cogswell, M., Parikh, D., and Batra, D. Grad-cam: Why did you say that? visual explanations from deep networks via gradient-based localization. *CoRR*, abs/1610.02391, 2016. URL <http://arxiv.org/abs/1610.02391>.
- Titensky, J. S., Jananthan, H., and Kepner, J. Uncertainty propagation in deep neural networks using extended kalman filtering. *CoRR*, abs/1809.06009, 2018. URL <http://arxiv.org/abs/1809.06009>.
- Touvron, H., Cord, M., Douze, M., Massa, F., Sablayrolles, A., and Jégou, H. Training data-efficient image transformers & distillation through attention. *CoRR*,

abs/2012.12877, 2020. URL <https://arxiv.org/abs/2012.12877>.

Tu, Z., Talebi, H., Zhang, H., Yang, F., Milanfar, P., Bovik, A., and Li, Y. Maxvit: Multi-axis vision transformer, 2022. URL <https://arxiv.org/abs/2204.01697>.

Vaswani, A., Shazeer, N., Parmar, N., Uszkoreit, J., Jones, L., Gomez, A. N., Kaiser, L., and Polosukhin, I. Attention is all you need. *CoRR*, abs/1706.03762, 2017. URL <http://arxiv.org/abs/1706.03762>.

Wang, L., Lin, Z. Q., and Wong, A. Covid-net: a tailored deep convolutional neural network design for detection of covid-19 cases from chest x-ray images. *Scientific Reports*, 10(1):19549, Nov 2020. ISSN 2045-2322. doi: 10.1038/s41598-020-76550-z. URL <https://doi.org/10.1038/s41598-020-76550-z>.

Wong, A. Netscore: Towards universal metrics for large-scale performance analysis of deep neural networks for practical usage. *CoRR*, abs/1806.05512, 2018. URL <http://arxiv.org/abs/1806.05512>.

Wong, A., Wang, X.-Y., and Hryniowski, A. How much can we really trust you? towards simple, interpretable trust quantification metrics for deep neural networks. *CoRR*, abs/2009.05835, 2020. URL <https://arxiv.org/abs/2009.05835>.

Yuan, Z., Yan, Y., Sonka, M., and Yang, T. Robust deep AUC maximization: A new surrogate loss and empirical studies on medical image classification. *CoRR*, abs/2012.03173, 2020. URL <https://arxiv.org/abs/2012.03173>.